Title: Rational design of adjuvants for subunit vaccines: the format of cationic adjuvants affects the induction of antigen-specific antibody responses

Authors: Giulia Anderluzzi[1†], Signe Tandrup Schmidt[1,2†], Robert Cunliffe[1], Stuart Woods[1], Craig W. Roberts[1], Daniele Veggi[3], Ilaria Ferlenghi[3], Derek T. O'Hagan[4], Barbara C. Baudner[3] and Yvonne Perrie[1]

[1]Strathclyde Institute of Pharmacy and Biomedical Sciences, University of Strathclyde, Glasgow, G4 0RE, UK

[2]Department of Infectious Disease Immunology, Center for Vaccine Research, Statens Serum Institut, Artillerivej 5, 2300 Copenhagen S, Denmark

[3]GSK, Siena, Italy.

[4]GSK, Rockville, United States

†These authors contributed equally

Key Words: Cationic delivery systems, protein subunit, vaccine adjuvant, antigen processing, pharmacokinetics, antibody response

Corresponding author:

Professor Yvonne Perrie
Strathclyde Institute of Pharmacy and Biomedical Sciences,
161 Cathedral St,
University of Strathclyde,
Glasgow, G4 0RE
Scotland.
yvonne.perrie@strath.ac.uk

Abstract

A range of cationic delivery systems have been investigated as vaccine adjuvants, though few direct comparisons exist. To investigate the impact of the delivery platform, we prepared four cationic systems (emulsions, liposomes, polymeric nanoparticles and solid lipid nanoparticles) all containing equal concentrations of the cationic lipid dimethyldioctadecylammonium bromide in combination with the Neisseria adhesin A variant 3 subunit antigen. The formulations were physico-chemically characterized and their ability to associate with cells and promote antigen processing (based on degradation of DQ-OVA, a substrate for proteases which upon hydrolysis is fluorescent) was compared *in vitro* and their vaccine efficacy (antigen-specific antibody responses and IFN-γ production) and biodistribution (antigen and adjuvant) were evaluated *in vivo*. Due to their cationic nature, all delivery systems gave high antigen loading (> 85%) with liposomes, lipid nanoparticles and emulsions being < 200 nm, whilst polymeric nanoparticles were larger (~350 nm). *In vitro,* the particulate systems tended to promote cell uptake and antigen processing, whilst emulsions were less effective. Similarly, whilst the particulate delivery systems induced a depot (of both delivery system and antigen) at the injection site, the cationic emulsions did not. However, out of the systems tested the cationic emulsions induced the highest antibody responses. These results demonstrate that while cationic lipids can have strong adjuvant activity, their formulation platform influences their immunogenicity.

Introduction

A wide range of particulate and nanoparticulate systems have been investigated as vaccine adjuvants. Within licensed formulations, emulsions [e.g. MF59 (1, 2) and AS03 (3)] and lipid-based particles [e.g. virosomes (such as Epaxal and Inflexal) and AS01 (4)] have been applied for many different vaccines applications. Polymeric based particles have also been investigated [e.g. (5)], in particular those using poly(lactide-co-glycolic acid) (PLGA) due to its biocompatible and biodegradable properties. Unfortunately, the harsh conditions normally required to entrap antigens within the polymeric nanoparticle can present issues [e.g. (6)], although modern manufacturing methods such as microfluidics can address this (7, 8).

The strategy of using cationic particles as adjuvants is widely reported as a means to increase the clinical potential of antigens, which are often poorly immunogenic on their own. For example, cationic adjuvants have been explored for both local and systemic administration (9-11) and a broad range of cationic lipids has been screened aiming to optimize formulation performance (12, 13). Due to their cationic nature, these adjuvants can electrostatically adsorb anionic antigens (including sub-unit proteins and nucleic based encoded antigens), thus protecting them against degradation and promoting uptake by professional antigen presenting cells (14, 15). Among the cationic lipids tested, dimethyldioctadecylammonium bromide (DDA), which was first tested for its immunological properties by Gall et al (16), has been used in a number of vaccine adjuvant formulations (14, 17, 18). The ability of DDA to associate antigens (19), prolong the deposition of the antigen at the injection site (18), and to enhance antigen cellular internalization (mainly through active actin-dependent endocytosis (20)), has been widely reported. DDA liposomes incorporating the immunostimulatory glycolipid trehalose dibehenate (TDB) (CAF01), have been used as an adjuvant for human tuberculosis (TB) vaccine in phase I clinical trials (21). Similarly, liposomes composed of DDA, monomycoloyl glycerol analogue 1 (MMG) and polyinosinic:polycytidylic acid [poly(I:C)], are currently being tested in humans (NCT03715985, NCT03412786). Building on these previous findings, we selected DDA as the cationic lipid component for four different vaccine adjuvant platforms.

In addition to liposomes, other cationic formulations have been considered including emulsions, polymeric nanoparticles (PNPs) and solid lipid nanoparticles (SLNs). For instance, a positively charged version of MF59 (a cationic nanoemulsion) has been shown to be particularly efficient for nucleic acid based vaccines against respiratory syncytial virus (RSV), cytomegalovirus (CMV) and

human immunodeficiency virus (HIV) (22, 23), and it is currently being evaluated in a Phase I clinical trial in humans (NCT04062669). With respect to polymeric nanoparticles, although cationic polymers such as polyethyleneimine (PEI) or ε-Poly-L-lysine (εPL) have been considered (24), the use of more biocompatible and less toxic cationic lipids in association with biodegradable polymers are preferred. For example, PLGA:DDA hybrid nanoparticles have been explored for *mycobacterium tuberculosis* HspX/EsxS fusion protein (25). In addition, therapeutically relevant peptides (e.g. calcitonin, cyclosporine A, insulin, LHRH, somatostatin) or protein antigens (e.g. hepatitis B and malaria antigens) have also been delivered using cationic solid lipid nanoparticles, with enhanced drug release kinetics, protein stability and *in vivo* performance (26-29). However, currently the only licenced solid lipid nanoparticle formulations are for cosmetic use (e.g. NanoRepair Q10, Dr. Rimpler) (30, 31).

Considering the variety of options in terms of delivery platforms, the aim of this work was to explore whether the format of the adjuvant might influence *in vitro* and *in vivo* functionality of subunit antigens. To achieve this, we prepared a panel of four cationic formulations, emulsions, liposomes, polymeric nanoparticles and solid lipid nanoparticles, which represents different classes of nanosized delivery systems. All were prepared incorporating the cationic lipid DDA as immunopotentiator. These systems were investigated in combination with Neisseria adhesin A variant 3 (NadA3), a soluble recombinant protein included in the Bexsero vaccine, which is a licensed multicomponent vaccine against serogroup B *Neisseria meningitidis* (MenB) (32). NadA acts through host epithelial cell adhesion and may influence colonization and invasion (33). NadA is a homotrimeric autotransporter adhesin consisting of an N-terminal globular domain connected by a coiled-coil stalk to a C-terminal integral membrane β-barrel that anchors the protein to the outer membrane and NadA is able to induce high titres of bactericidal antibodies (34, 35). Data from the crystal structure of the 24-170 NadA3 fragment at 2.45 Å resolution (36), together with detailed mapping of the binding sites of human bactericidal antibodies and cell-based assays data, provide deep knowledge of the 4CMenB vaccine component and of its biological mechanism of action, suggesting NadA3 as a useful antigen to test the potential of our newly formulated DDA-based adjuvants.

Materials and methods

Materials

Poly (D, L-lactide-co-glycolide) lactide: glycolide (50:50) (PLGA), mol wt 30,000-60,000, dimethyl sulfoxide (DMSO), tristearin (Grade II-S, ≥90%), phosphate-buffered saline (PBS), skim milk, penicillin-streptomycin, L-glutamine solution, concanavalin A, bovine serum albumin (BSA), sulphuric acid, pontamine blue and squalene were obtained from Sigma-Aldrich Ltd. 1,2-dioleoyl-sn-glycero-3-phosphoethanolamine (DOPE) and dimethyldioctadecylammonium bromide (DDA) were obtained from Avanti Polar Lipids. 1,1'-dioctadecyl-3,3,3',3'-tetramethylindodicarbocyanine (DiD), ethanol, methanol, DQ Ovalbumin, Tween 80 and Span 85 were obtained from Thermo Fisher, and TRIS Ultra-Pure was obtained from MP Biomedicals. Roswell Park Memorial Institute 1640 medium (RPMI-1640) was purchased from Invitrogen. Foetal bovine serum was obtained from Gibco. Dihydroxyvitamin D3 was obtained by Enzo Life Sciences. 3,3',5,5'-tetramethylbenzidine (TMB) was obtained from Kem-En-Tec. Anti-mouse IgG antibody, anti-mouse IgG1 antibody, anti-mouse IgG2a antibody, biotin-conjugated anti-mouse IFN-γ, and streptavidin-conjugated horseradish peroxidase (HRP) were acquired from BD Biosciences. Cholesterol, [1,2-3H(N)]-, 1 mCi (37 MBq) and Ultima Gold were obtained from Perkin Elmer. Trehalose and hydrogen peroxide30% v/w were purchased from Acros Organics.

NadA3 purification and labelling with fluorophore

NadA3 protein was expressed as a His-tag fusion in *E. coli* BL21 (DE3) cells (New England Biolabs). Cell pellets were resuspended in binding buffer (300 mM sodium chloride, 50 mM sodium phosphate, pH 8) and lysed by sonication (Qsonica Q700) with 5 cycles of 30 seconds of sonication (40% amplitude) interspersed with 1 minute on ice. Cell lysates were clarified by ultracentrifugation at 36200 x g for 45 minutes and then affinity chromatography was performed at room temperature using a HisTrap HP 5 mL linked to an AKTAPurifier (GE Healthcare), with the protein being eluted by employing an imidazole gradient. Size-exclusion chromatography was then performed using a HiLoad 16/600 superdex 75 pg column (GE Healthcare), equilibrated in binding buffer. The quality of the final NadA3 sample was checked by gel electrophoresis using NuPAGE Novex Bis-Tris 4-12 % gels ran in MES buffer then stained with SimplyBlue SafeStain (ThermoFisher). Fractions were then pooled and filtered using a Millex 0.22 µM filter. A BCA assay using a Pierce BCA Protein Assay Kit (ThermoFisher) was performed to determine the protein concentration. The infrared fluorescent

Alexa Fluor 790 label was conjugated to NadA3 using an Alexa Fluor 790 Antibody Labelling Kit (Thermo Scientific) following manufacturer's instructions.

Preparation of emulsions

Emulsions were prepared as previously described by Ott et al., (37), with some modifications. Briefly, to prepare oil in water emulsions, squalene (5.0%, w/w), DDA (4.3% w/w), and Span 85 (0.5%, w/w) were combined and heated to 65 °C. The resulting oil phase was then mixed with an aqueous phase consisting of Tween 80 in Tris buffer (10 mM, pH 7.4) and vortexed for 1 min to provide a homogeneous feedstock. This primary emulsion was sonicated for 15 min (Bioruptor Plus, Diagenode) to reduce the droplet size.

Preparation of liposomes, polymeric nanoparticles and solid lipid nanoparticles

Liposomes, polymeric nanoparticles and solid lipid nanoparticles were prepared in the NanoAssemblr Platform (Precision NanoSystems Inc) as previously described by (38), but with some modifications. In essence, to prepare cationic liposomes, lipid mixtures composed of DOPE and DDA (1:1 w/w) were dissolved in methanol. Tris buffer (10 mM, pH 7.4) was used as the aqueous phase. To manufacture cationic polymeric nanoparticles, PLGA and DDA (1:1 w/w) were dissolved in DMSO and acetate buffer (100 mM, pH 6) was used as the aqueous phase. To prepare cationic solid lipid nanoparticles, tristearin and DDA 1:1 (w/w) were dissolved in ethanol at 70°C. Tris buffer (10 mM, pH 7.4) was used as aqueous phase. All formulations were prepared using a staggered herringbone micromixer. The total flow and the aqueous to organic phase ratio were set to 10 mL/min and 1:1, respectively. To remove residual solvent, the formulations were dialysed for 1 hour at room temperature against the same formulation (dialysis membrane cut off 14000 Da).

Protein complexation

NadA3 was electrostatically complexed to the various adjuvants (emulsions, liposomes, polymeric nanoparticles and solid lipid nanoparticles) at 1:30 w/w protein to cationic lipid ratio. NadA3 was added dropwise to either liposomes, solid lipid nanoparticles, polymeric nanoparticles or emulsions under mild stirring and allowed to complex at 4°C overnight. Each final formulation contained 3 mg/mL of DDA and 100 µg/mL of NadA3. Prior to *in vivo* administration, 10% (w/v) trehalose was added to formulations to maintain isotonicity upon injection.

Evaluation of antigen binding efficiency

To evaluate the NadA3 adsorption efficiency to the different adjuvants, 500 µL of formulations were centrifuged for 20 min at 10,000 rpm using a Beckman Coulter Airfuge Air-Driven Ultracentrifuge (Brea, CA, USA) to pellet the adjuvants. The supernatant was removed and the absorbance of unbound NadA3 was measured at 280 nm using a Nanodrop 2000c (Thermo Scientific). NadA3 quantification was achieved by referring to a linear calibration curve (R^2=0.999), with limit of detection (LOD) and limit of quantification (LOQ) of 3.8 and 11.5 µg/mL, respectively.

Physiochemical characterization of formulations

All formulations were characterized in terms of hydrodynamic particle size (Z-average), polydispersity index (PDI) and zeta potential by dynamic light scattering (DLS) with a Zetasizer Nano ZS (Malvern Panalytical, Malvern, UK) at 0.1 – 0.2 mg/mL at 25 ˚C in either TRIS buffer (10 mM, pH 7.4) or acetate buffer (100 mM, pH 6).

***In vitro* studies**

To track cellular association, adjuvants were co-formulated with the lipophilic fluorescent dye DiD (0.1% w/v) added in the lipid mixture prior to microfluidics mixing or emulsification. The association of the adjuvants and degree of protein antigen processing (based on degradation of DQ-OVA) were evaluated *in vitro* in THP-1 cells. DQ-OVA was used to measure protein degradation; DQ-OVA is a substrate for proteases and upon hydrolysis is fluorescent. THP-1 cells were cultured in RPMI 1640 supplemented with 10% (v/v) Foetal Bovine Serum, 1% (v/v) Penicillin-Streptomycin and 1% (v/v) L-glutamine solution and stimulated with 100 nM dihydroxyvitamin D3 for 48 hours. The adjuvants were prepared by mixing 100 µL DiD-labelled adjuvants with 10 µg DQ-OVA and Tris-buffer (10 mM, pH 7.4) *ad* 200 µL. 20 µL of this mixture was subsequently diluted in 1.5 mL RPMI 1640. As controls, RPMI 1640 and DQ-OVA in RPMI 1640 were used. The THP-1 cells at 2 x 10^5 cells/mL were seeded and mixed with the diluted adjuvants (20 µg/mL) or controls and incubated at 37°C, 5% CO_2. Samples were removed at 0, 30, 60, 120, 180 and 240 minutes post incubation, washed in PBS and fixated in 4% paraformaldehyde prior to flow cytometry analysis on an AttuneNxt flow cytometer (Invitrogen). The fluorophores were detected at ex./em. 488/530 nm for DQ-OVA and ex./em. 638/670 nm for DiD, and the data was analysed using FlowJo v10 (BD).

In vivo studies

All *in vivo* studies adhered to the 1986 Scientific Procedures Act (UK project license number PPL3003289/ personal license number IC2992F8F). All protocols have been subject to ethical review and were carried out in a designated establishment following ARRIVE guidelines.

Biodistribution of radiolabeled cationic formulations

Groups of four female 6–8-week-old BALB/c mice (20-25 g) were housed appropriately and given a standard mouse diet ad-libitum. To track their biodistribution, emulsions, liposomes, PNPs and SLNs were co-formulated with the radioactive label ^{3}H-cholesterol, added in the lipid mixture prior to microfluidics mixing or emulsification as previously described (39, 40). To provide isotonicity, trehalose was added to a final concentration of 10% (w/v). Each dose (50 µL) contained 25 µg of DDA and 25 ng of ^{3}H-cholesterol corresponding to 200 KBq/dose. Three days before injection, mice were injected with 200 µL of pontamine blue (0.5 % w/v) subcutaneously (s.c.) into the neck scruff as a marker for lymph nodes. Mice were injected intramuscularly in the right quadriceps then euthanized at 6, 24 and 48 hours post injection (p.i). The spleen, liver, right quadriceps and draining lymph nodes [popliteal lymph node (PLN) and inguinal lymph node (ILN)], and the remaining carcass were collected for analysis and digested following previous protocols (39). Briefly, solubilized completely in 10M NaOH (2 mL) at 60 °C overnight and subsequently bleached with 30% w/v hydrogen peroxide (200 µL) for 2 h at 60°C. 10 mL of Ultima Gold Scintillation cocktail was then added to each sample and the radioactivity was quantified by using Liquid Scintillation Analyser Tri-Carb 2810 TR (Perkin Elmer). The ratio of injected dose recovered in each organ was calculated with respect to the original dose.

Biodistribution of NadA3 adsorbing formulations

The biodistribution of DiD-labelled adjuvants was evaluated by using *in vivo* imaging. Female BALB/c mice bred in-house, 7-9 weeks old, were divided in groups of 3. One additional naïve mouse was used as a negative control to establish the background levels at each time point. The mice were administered 10 µg/dose AF790-labelled NadA3 either unadjuvanted or adjuvanted with DiD-labelled liposomes, solid lipid nanoparticles, polymeric nanoparticles and emulsions in 50 µL injected intramuscularly (i.m.) in the right quadriceps. Immediately after immunization, the mice were anaesthetized using 3% isoflurane, and imaged under maintenance anesthetics in the IVIS Spectrum In Vivo Imaging System (Perkin Elmer). All mice were imaged first with the DiD filter (ex./em. 605/680 nm) and subsequently with the AF790 filter (ex./em. 745/820 nm) at 0.2 s

exposure time, binning factor 4 or 8 and f number 2 or 8, including the control mouse. The control mouse results were used to establish that the background levels remained constant throughout the study. Imaging sessions were repeated at day 1, 2, 3, 4, 7, 9 and 11 p.i., after which the study was terminated. Imaging data was analyzed using Living Image software (Perkin Elmer).

In vivo evaluation of adjuvant immunogenicity

An *in vivo* study was performed to evaluate the induction of antigen specific immune responses following immunization with NadA3 combined with different cationic adjuvants (liposomes, solid lipid nanoparticles, polymeric nanoparticles and emulsions, respectively). Male BALB/c mice aged 7-9 weeks were housed in study groups and allowed free access to food and water. The mice were immunized i.m. with 50 µL in both quadriceps at day 1 and 28 with a total dose of 10 µg NadA3 either unadjuvanted or adjuvanted with 0.6 mg/dose of liposomes, solid lipid nanoparticles, polymeric nanoparticles and emulsions. Mice were euthanized at day 14 after the final immunization, and the blood and spleen were collected. The serum was collected from the blood, while single cell suspensions were obtained from the spleens. Briefly, the spleens were processed by using a metal mesh cell strainer followed by two washes with RPMI 1640. The splenocytes were resuspended in RPMI 1640 supplemented with 10% (v/v) Foetal Bovine Serum, 1% (v/v) Penicillin-Streptomycin and 1% (v/v) L-glutamine solution. The cells (2 x 10^6 cells/mL) were stimulated with 2 µg/mL NadA3 at 37°C, 5% CO_2 for four days with media and concanavalin A (5 µg/mL) wells as negative and positive controls, respectively. The supernatants were collected and stored at -20°C. To ensure intra-study variation was considered, two studies were conducted (2-3 mice per group) and the results were combined in the analysis of the data.

The levels of total antigen-specific IgG, IgG1 and IgG2a in the serum were determined by using ELISA. The Maxisorb plates (Nunc) were coated overnight at 4°C with 2 µg/mL NadA3 in carbonate buffer, followed by a blocking step with 2% bovine serum albumin (BSA) in phosphate-buffered saline (PBS) for 1.5 hours at room temperature. The serum samples were serially diluted and the plates were incubated at room temperature for 2 hours, followed by 1 hour incubation with horseradish peroxidase (HRP) conjugated anti-mouse IgG, anti-mouse IgG1, or anti-mouse IgG2a. The plates were developed by using 3,3',5,5'-tetramethylbenzidine (TMB), and the reaction was stopped with 0.2 M sulphuric acid. The plates were read at 450 nm with 620 nm correction.

The levels of IFN-γ in the stimulated splenocyte supernatants were determined by using ELISA. The Maxisorb plates were coated overnight at 4°C with anti-mouse IFN-γ antibodies in carbonate buffer, followed by a blocking step with 2% skim milk in PBS for 1.5 hours at room temperature. The supernatants were diluted 8-fold in 2% BSA in PBS, and the plates were incubated at room temperature for 2 hours, followed by 1 hour incubation with biotin-conjugated anti-mouse IFN-γ antibodies. This was followed by 30 min incubation with streptavidin-conjugated HRP. The plates were developed by using TMB, and the reaction was stopped with 0.2 M sulfuric acid. The plates were read at 450 nm with 620 nm correction.

Data analysis

For the biodistribution study, captured images were analysed using the Living Image 4.1 software (PerkinElmer Inc.). The fluorescence signal data were in all cases corrected by subtracting the signal detected in the control mouse that had not been immunised with a fluorescent marker. Fluorescent signal data from all tissues were obtained considering the lateral view. All captured fluorescence signals obtained were expressed as the radiance, technically defined as fluorescence emission radiance per incident excitation intensity: photons/s/cm^2/sr (steradian). The endpoint titers for the total IgG, IgG1 and IgG2a levels were calculated for the collected data from the repeated animal studies. The method described by Frey et al was used to calculate the cutoff values for each dilution point with unadjuvanted NadA3 as the control (41). Statistical analysis of the log values of the calculated endpoint titers was performed using Brown-Forsythe and Welch ANOVA assuming non-equal standard deviations (Prism 8, Graphpad).

Results

NadA3 adsorbing DDA-based adjuvants were all nanosized, cationic and with high antigen loading

Four vaccine delivery platforms were prepared (emulsions, liposomes, polymeric nanoparticles and solid lipid nanoparticles) each containing equal concentrations of the cationic lipid DDA (3.0 mg/mL). Prior to addition of the subunit antigen (NadA3), the emulsions were 110-150 nm in size, with low polydispersity (<0.2) and a positive surface charge with a zeta potential of 28 ± 2 mV (Table 1). In contrast, the liposomes, polymeric nanoparticle and solid lipid nanoparticles were smaller in size (40 - 70 nm), but again with low polydispersity (<0.3) and cationic zeta potentials (40 – 60 mV) (Table

1). When the antigen was added to these formulations, NadA3 association was high (>85%; Table 1). On addition of the antigen, the particle size and PDI of all four formulations increased and the zeta potential was reduced, as a result of complexation between the cationic formulations and the anionic antigen (Table 1).

Table 1. Physicochemical properties of DDA-based formulations. Chemical composition, size (z-average), polydispersity index (PDI), zeta potential (ZP) and NadA3 adsorbance efficiency (A. E.) of DDA-based emulsions, solid lipid nanoparticles, polymeric nanoparticles and liposomes either in presence or in absence of 100 μg/mL of NadA3 antigen. DDA: Dimethyldioctadecylammonium bromide, PLGA: poly(lactic-co-glycolic acid), DOPE: dioleoylphosphatidylethanolamine. Results are represented as mean ± SD of three independent measurements, * $p \leq 0.05$ significance between formulations prepared with and without NadA3.

Delivery system	Chemical composition (mg/mL)	NadA3 protein (μg/mL)	Size ± SD (d.nm)	PDI ± SD	ZP ± SD (mV)	NadA3 A.E. ± SD (%)
Emulsions	Squalene: 3.5 DDA: 3.0 Span 85: 0.3 Tween 80: 0.3	0	131 ± 18	0.18 ± 0.02	28 ± 3	-
		100	187 ± 6*	0.22 ± 0.02	19 ± 2*	92 ± 2
Liposomes	DOPE: 3.0 DDA: 3.0	0	41 ± 4	0.25 ± 0.01	56 ± 4	-
		100	111 ± 4*	0.39 ± 0.01*	37 ± 2*	95 ± 2
Polymeric nanoparticles	PLGA: 3.0 DDA: 3.0	0	38 ± 3	0.11 ± 0.03	53 ± 2	-
		100	356 ± 81*	0.17 ± 0.03	41 ± 7*	95 ± 1
Solid lipid nanoparticles	Tristearin: 3.0 DDA: 3.0	0	66 ± 2	0.15 ± 0.03	4 3 ± 5	-
		100	154 ± 4*	0.37 ± 0.02*	31 ± 5*	85 ± 1

The format of the cationic adjuvant influences cellular association and antigen processing *in vitro*

Given that the four formulations were shown to offer high antigen loading, the next step was to assess their ability to deliver antigen to antigen presenting cells and promote antigen presentation. To achieve this, DiD-labelled adjuvants were prepared to measure cell association with VD3-stimulated THP-1 cells. To consider antigen processing, antigen degradation was measured using chicken egg ovalbumin conjugated to the BODIPY FL dye (DQ-OVA), a self-quenching reporter that

fluoresces at proteolytic degradation of the protein, was incorporated within the adjuvant formulations (Figure 1). The level of protein degradation correlated with the increase in fluorescence intensity.

The degree of cellular association of the adjuvants, expressed as percentage of DiD positive cells, was time dependent (Figure 1A); for the emulsions, the percentage of DiD positive cells increased up to 20% after 240 min (Figure 1A). In contrast, with the liposomes, polymeric nanoparticles and solid lipid nanoparticles, there was a rapid cell association (between 40 to 50% DiD^+ cells) after only 1 min, followed by a slower increase until 60 min, and subsequently a plateau of 40 to 80% DiD^+ cells was reached (Figure 1A). Similar results were obtained when the degree of association was expressed as mean fluorescence intensity (MFI) with the emulsions showing low MFI compared to the liposomes, polymeric nanoparticles and solid lipid particles, which were almost 6 fold higher than the emulsions (Figure 1B). To assess if the size of the particles might affect their interaction with cells, THP-1 uptake was also analyzed in terms of relative number of particles (Nr) which is proportional to the MFI normalized by particles volume. As expected, emulsions had the lowest Nr due to the lowest MFI (Figure 1C). However, the effect of formulation attributes on cell association was more evident between the other three formulations; the number of associated liposomes, which had the smallest size (111 ± 2 nm; Table 1), was 3-fold and 30-fold higher than solid lipid nanoparticles (154 ± 4 nm; Table 1, $p \leq 0.05$) and polymeric nanoparticles (354 ± 85 nm; Table 1, $p \leq 0.05$) respectively (Figure 1).

When considering antigen degradation, the percentage of DQ-OVA positive cells followed a similar trend to cell association (Figure 1D, E and F). At levels comparable to the non-adjuvanted DQ-OVA control, poor antigen degradation was promoted by emulsions when calculated in terms of both DQ-OVA positive cells (Figure 1D) and DQ-OVA MFI ((Figure 1E). However, co-delivery of DQ-OVA with liposomes, polymeric nanoparticles and solid lipid nanoparticles showed a substantial increase in percentage of DQ-OVA positive cells especially at the earliest time points, implying a marked amount of protein degradation occurred within 60 minutes. When data was expressed as DQ-OVA MFI, similar to cell association, there was no significant difference between liposomes, polymeric nanoparticles and solid lipid nanoparticle (MFIs between 1500 and 2000), while emulsions showed the lowest MFI, which was similar to that of unformulated DQ-OVA (Figure 1E, $p \leq 0.05$). The link between cell association and antigen processing is shown in Figure 1F, where % cell association (from Figure 1A) is plotted against % antigen degradation (from Figure 1D) for all time points; emulsions showed low cell association and antigen degradation whilst the solid lipid nanoparticles

had high cell association and high antigen degradation. In general, the efficiency of promoting antigen degradation by THP-1 cells was ranked in the order solid lipid nanoparticles > polymeric nanoparticles ≈ liposomes > emulsions.

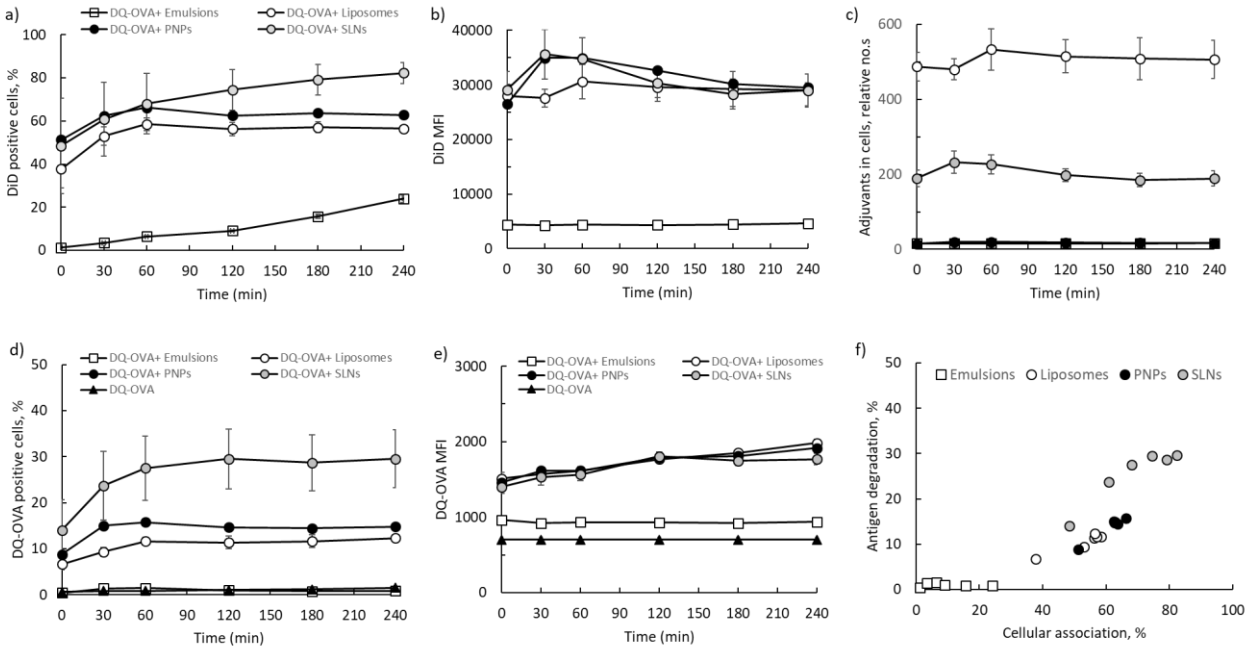

Figure 1. *In vitro* association of adjuvants with THP-1 cells and induction of antigen degradation. Association efficiency of emulsions, liposomes, polymeric nanoparticles (PNPs) or solid lipid nanoparticles (SLNs) expressed as A) Percentage of DiD^+ cells, B) DiD mean florescence intensity (MFI) or C) Relative number of associated adjuvants (Nr). Antigen degradation efficiency of emulsions, liposomes, PNPs or SLNs is expressed as D) DQ-OVA^+ cells and E) DQ-OVA mean fluorescence intensity (MFI). F) Plots the % of cell association versus % antigen degradation at all time points measured (data from A and D). Results are represented as mean ± SD of three independent experiments. Refer to Figure S1 in the supplementary for representative histograms of DiD and DQ-OVA positive THP-1 cells incubated with different adjuvants.

The format of the cationic adjuvant affects clearance of both adjuvant and antigen from the injection site.

Given that increased levels of antigen degradation increased with cell association, the degree of retention/depot formation at the injection site promoted by the four different formulations was then investigated. Fluorescently labelled antigen (AF790-NadA3) adjuvanted with DiD-labelled formulations were injected i.m. in the right quadriceps and their biodistribution was tracked over 11 days by using IVIS (Figure 2, 3, S1 - 3). Herein, only data for the injection site (Figure S4) and kidneys (Figure S4) are reported as no signal from other organs, like liver, spleen, lung or heart was detected. Although the total flux did not show appreciable variability among formulations over time

(Figure 2A), differences were evident when values were normalized and expressed as percentage of signal ratio (Figure 2B). Though all groups were injected with the same dose of fluorescently labelled adjuvant and antigen, different initial levels of fluorescence intensity were detected in mice receiving emulsions compared to the other adjuvants (Figure 3A). This may be due the way the dyes are arranged within the adjuvant; emulsions have a relatively large oil-phase compartment, where the DiD dye can be dissolved, whereas for the other adjuvants the dye is incorporated within the lipid membrane and exposed to the aqueous phase. Similarly, the location of the antigen within the formulation and any subsequent quenching effect may influence the initial level of antigen and this could affect the measured absolute fluorescence intensity among the four formulations.

The emulsions drained rapidly from the injection site (approximately 20% of the initial dose remaining after 24 hours), while liposomes, solid lipid nanoparticles and polymeric nanoparticles were retained in the quadriceps with more than 70% of the initial dose detected 11 days p.i. (Figure 2B). This indicates that cationic liposomes, polymeric nanoparticles and solid lipid nanoparticles formed a depot at the injection site, whereas the cationic emulsions did not. It might be worth noting that signal of liposomes, polymeric nanoparticles and solid lipid nanoparticles at day 1 was 2-fold higher than that measured at 1 h (Figure 2C). This could be due to self-quenching of DiD resulting from interaction between formulations and serum protein which could have led to immediate aggregation of cationic particles upon injection (42). The retention of the particles coincided with retention of the associated antigen (Figure 4). Again, variability of antigen distribution was more evident when represented as percentage of signal ratio (Figure 3B) rather than total flux (Figure 3A). The drainage pattern of NadA3 co-formulated with emulsions was similar to that of unadjuvanted NadA3, and both were cleared rapidly from the site of injection with between 30 and 40% of initial antigen dose present 24 hours p.i. (Figure 3B). In contrast, NadA3 adsorbed to cationic liposomes, polymeric nanoparticles and solid lipid nanoparticles drained more slowly from the quadriceps with almost all of the administered antigen dose detected at the injection site 24 hours p.i. (Figure 3B). As a consequence of the depot formation, the level of NadA3 adjuvanted with cationic liposomes, polymeric nanoparticles and solid lipid nanoparticles was still significantly ($p \leq 0.05$) higher at 11 days p.i. compared to unadjuvanted NadA3 or NadA3 adjuvanted with emulsions (Figure 3B). To consider the retention of the antigen promoted by the adjuvant, data from Figure 2B and 3B were plotted as the Area Under the Curve (AUC; flux.day) for both antigen and adjuvant (Figure 4). This confirms that the emulsion system does not promote a depot of antigen or adjuvant, whilst liposomes, polymeric nanoparticles and solid lipid nanoparticles induce

similar retention of antigen and adjuvant at the injection site with no significant difference among the three formulations, but all significantly higher than the emulsion and unadjvuanted antigen ($p \leq 0.05$). Despite adjuvant-dependent differences in NadA3 retention at the site of injection, the levels of NadA3 accumulation in the kidneys were similar across the study groups (Figure S4).

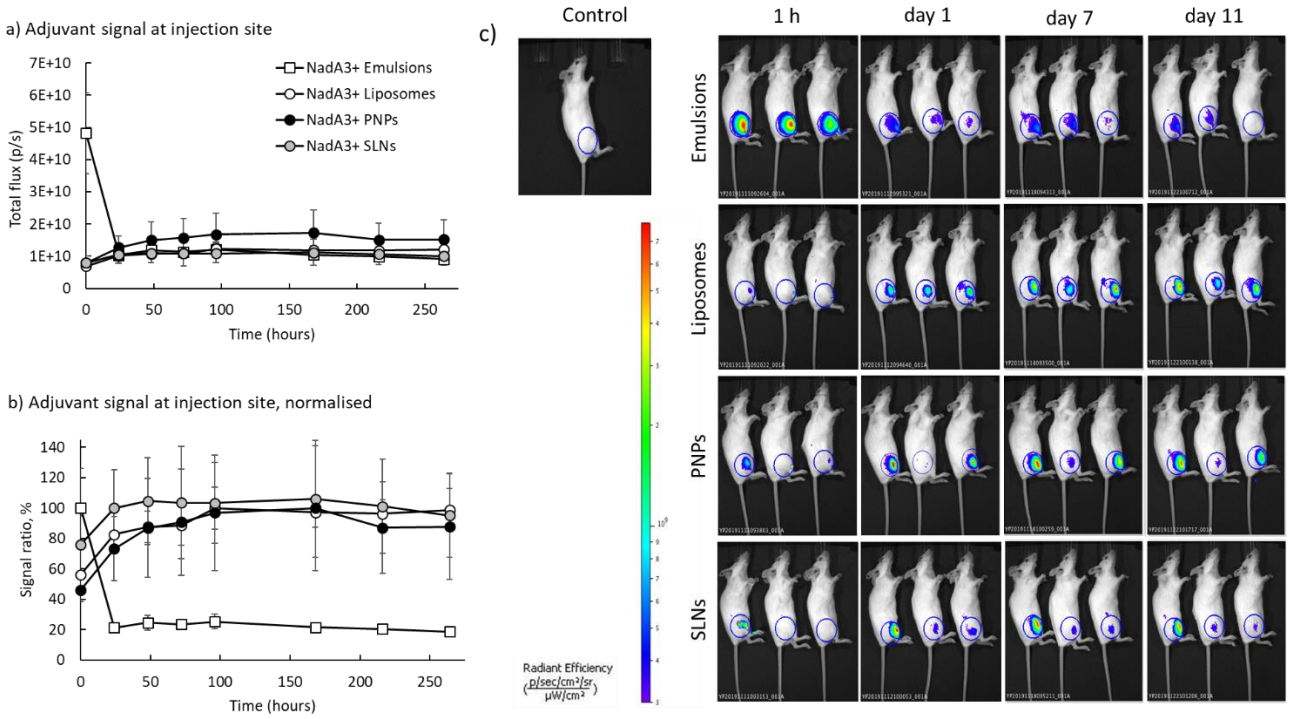

Figure 2. Biodistribution of DiD-labelled adjuvants in mice following intramuscular administration. Female BALB/c mice were administered NadA3 adjuvanted with DiD-labelled emulsions, liposomes, polymeric nanoparticles (PNPs) and solid lipid nanoparticles (SLNs) intramuscularly in the right quadricep. The fluorescent signals were evaluated by IVIS over 11 days p.i. A) Pharmacokinetic profiles of DiD-labelled adjuvants at the injection site. B) Results were normalized and replotted as percentage of signal ratio. C) Images acquired at selected time points. Dashed lines represent background level. Results are represented as the mean ± SD of three animals per group. Refer to Figure S2 in the supplementary for images of mice administered with adjuvanted NadA3 acquired at all time points over 11 days p.i.

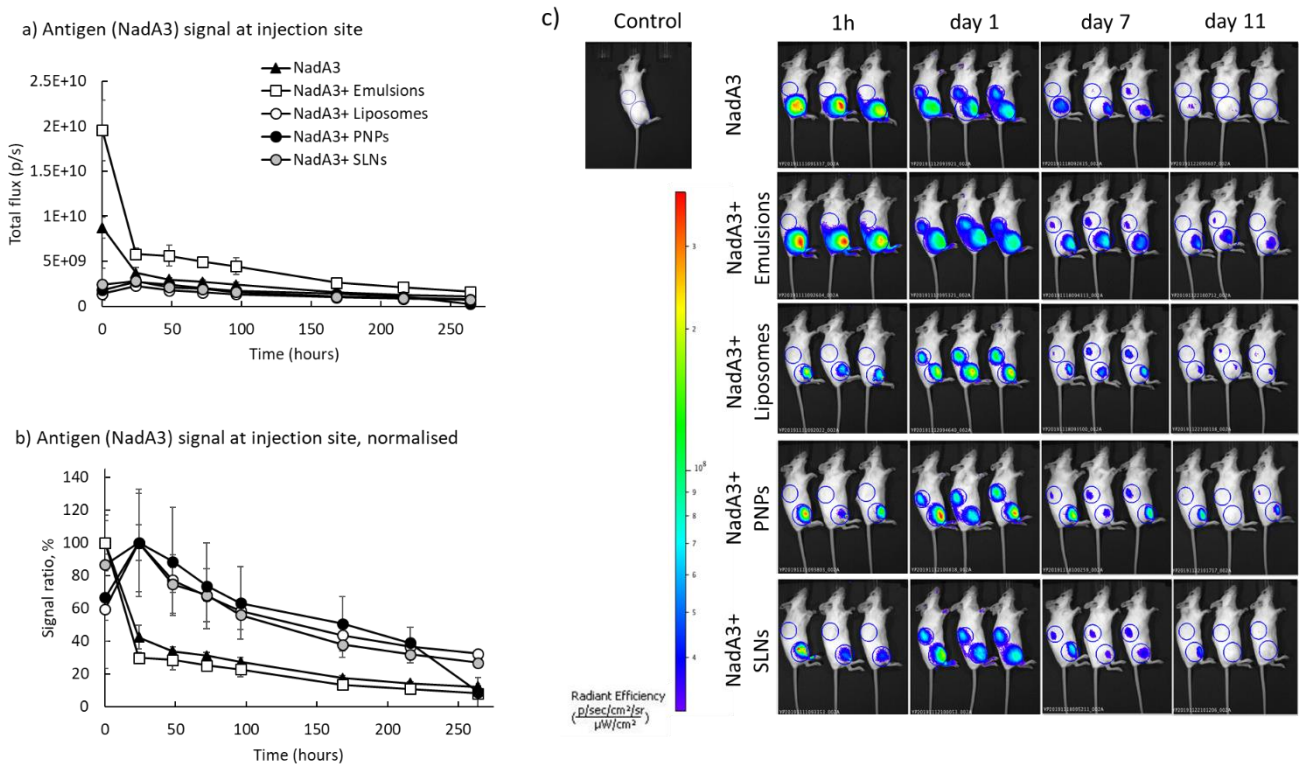

Figure 3. Biodistribution of adjuvanted NadA3 antigen. Female BALB/c mice were administered unadjvuanted AF790-labelled NadA3 or adjuvanted with DiD-labelled emulsions, liposomes, polymeric nanoparticles (PNPs) and solid lipid nanoparticles (SLNs) intramuscularly in the right quadricep. The fluorescent signals were evaluated by IVIS over 11 days p.i. A) Pharmacokinetic profiles of either unadjuvanted or adjuvanted NadA3 at the injection site. B) Results were normalized and replotted as percentage of signal ratio. C) Images acquired at selected time points. Results are represented as the mean ± SD of three animals per group. Dashed lines represent background level. Refer to Figure S3 in the supplementary for images of mice administered with either unadjuvanted or adjuvanted NadA3 acquired at all time points over 11 days p.i.

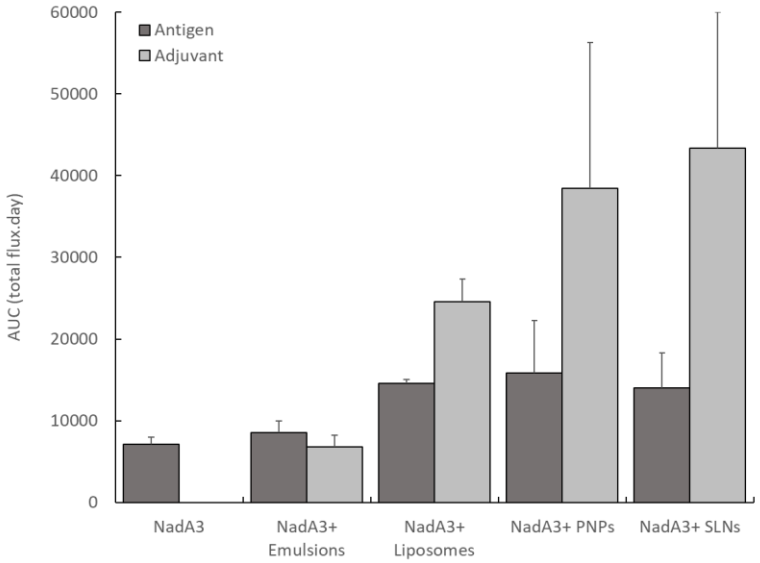

Figure 4. Comparison of AUC for both antigen and adjuvant after intramuscular injection. The retention of the antigen promoted by the adjuvant was calculated as area under the curve (AUC) for each formulation for both adjuvant and antigen (AUC; flux.day).

While the IVIS studies provided an overview of the biodistribution of the subunit vaccine components, we wished to further detail the biodistribution on an organ level. Therefore, we administered ^{3}H-cholesterol-labeled versions of the four formulations intramuscularly to BALB/c mice and their distribution was monitored over 48 h. The concentration of radio-label tracer was low enough not to affect the size and surface charge of the formulations (data not shown). All tested cationic delivery systems were retained at the injection site at various levels over the course of the study. However, emulsions drained from the muscle to a greater degree, especially compared to PNPs or SLNs 48 hours p.i. (Figure 5A).

When focusing on local draining lymph nodes, emulsions tended to reach the popliteal lymph node to a greater extent than liposomes, PNPs or SLNs (Figure 5B). At 24 hours the level of emulsions was approximately 3-fold higher than that of all the other formulations and this enhanced accumulation was maintained over 48 h p.i. (Figure 2B). Overall, the accumulation of formulations in the ILN was lower than in the PLN (a maximum of 0.25% vs 0.7% of initail dose detected respectively) and no significant differences across formulations in terms of percentage of dose was measured (Figure 5C).

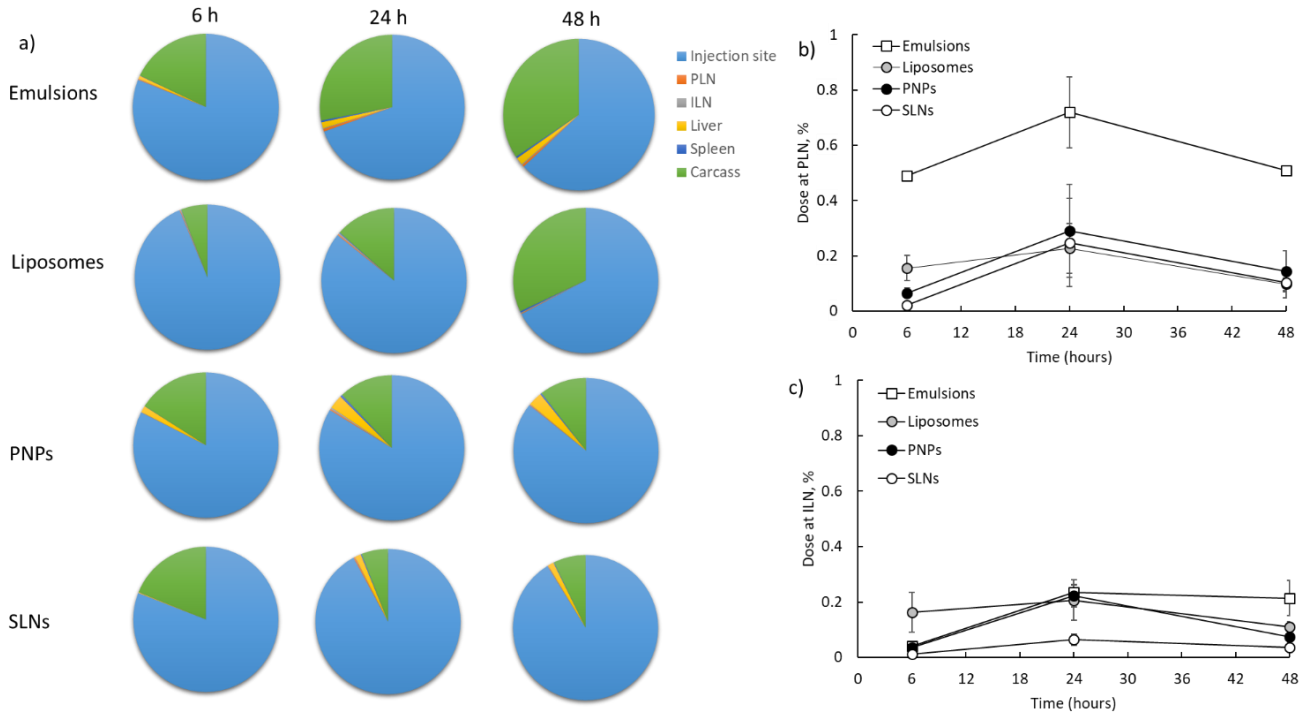

Figure 5. Biodistribution of radiolabeled cationic formulations. Female BALB/c mice were administered ^{3}H-cholesterol-labelled emulsions, liposomes, polymeric nanoparticles (PNPs) and solid lipid nanoparticles (SLNs) intramuscularly in the right quadriceps. The radioactivity was evaluated in the injection site, liver, spleen, popliteal lymph node (PLN), inguinal lymph node (ILN) and whole carcass over 48 hours p.i. A) Pharmacokinetic profiles of ^{3}H-cholesterol-labelled adjuvants. Percentage of dose determined at B) popliteal lymph node (PLN) and C) inguinal lymph node (ILN). Results are expressed as the mean ± SD of four animals. Data of biodistribution of liposomes were previously published by (43).

Antigen-specific antibody responses are dependent on the type of adjuvant

The immune responses induced by the cationic adjuvants in combination with the protein antigen NadA3 were evaluated in female BALB/c mice with two i.m. immunizations four weeks apart and termination at two weeks after the final injection (Figure 6). An antigen dose of 10 µg was used based on previous work on developing novel vaccine candidate for *Neisseria meningitides* using the NadA3 subunit (44).The type of adjuvant had a significant effect on the induction of antigen specific total IgG antibody responses (Figure 6 A, D). The highest endpoint titers were observed for the group immunized with NadA3 adjuvanted with the emulsion, whereas NadA3 adjuvanted with polymeric nanoparticles induced levels of antigen-specific IgG antibodies similar to the levels promoted by unadjuvanted NadA3. The immune responses were further analyzed for the induction of antigen-specific IgG1 and IgG2a antibodies. In correlation with the total IgG responses, the highest IgG1

endpoint titers were observed for the group immunized with NadA3 adjuvanted with the emulsion, whereas the lowest responses were induced by NadA3 adjuvanted with polymeric nanoparticles (Figure 6 B, E). The groups immunized with NadA3 adjuvanted with liposomes and solid lipid nanoparticles showed intermediate levels of antigen-specific IgG1 (Figure 6 B, E). The antigen-specific IgG2a responses were low for all adjuvants (Figure 6 C, F). Only NadA3 adjuvanted with the emulsion showed some induction of antigen-specific IgG2a. Accordingly, no antigen-specific IFN-γ responses were induced following immunization with NadA3 adjuvanted with any adjuvant (Figure S5). This indicates the antibody responses induced are strongly skewed towards a Th2-type response; however, it should be noted that BALB/c mice are a Th2-dominant mouse strain.

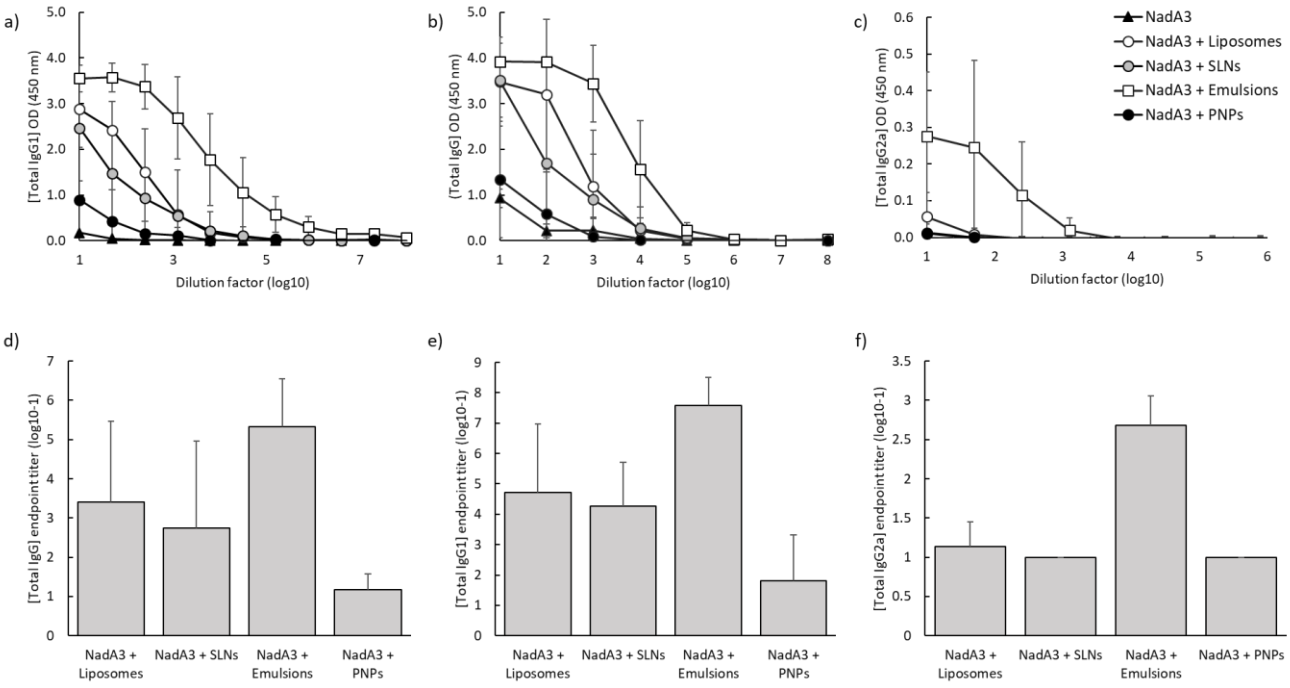

Figure 6. ***In vivo*** **humoral responses promoted by four different cationic delivery platforms.** Female BALB/c mice were immunized twice i.m. with unadjuvanted NadA3 (10 µg/dose) or NadA3 adjuvanted with cationic emulsions, liposomes, polymer nanoparticles (PNPs) and solid lipid nanoparticles (SLNs), with a booster immunization four weeks after the prime immunization. The antigen-specific total IgG, IgG1 and IgG2a levels in the blood were evaluated two weeks after the final immunization by using ELISA. Antigen specific A) total IgG levels, B) IgG1 and C) IgG2a average of mice in repeated studies, n=3-6, mean ± SD. The end point titers were calculated using the signal from the unadjuvanted NadA3-immunized group as background for D) total IgG, E) IgG1 and F) IgG2a, n=4-6, lines denote mean ± SD. $p \leq 0.05$ (*).

Discussion

The strategy of incorporating positively charged lipids into synthetic delivery systems is widely established to optimize immune response of otherwise poorly immunogenic or labile antigens (45, 46). A cationic surface charge enhances association of negatively charged antigens to lipid-based particles and promote cellular trafficking (47, 48). Moreover, direct mixing between non-ionizable lipids and proteins with isoelectric points (pI) below 7 results in spontaneous association at neutral pH (43). For example, it has been observed that CAF01 liposomes efficiently adsorbed OVA and bovine serum albumin (BSA), which both have pI at approximately 4.5, whereas lysozyme at pI 11 did not adsorb onto the cationic liposomes (49). Efficient delivery of subunit protein antigens is believed to be influenced by the degree of interaction between protein and the delivery system, either by entrapment or by surface adsorption (20). These findings correlated with data reported in the present study, where using highly positive DDA-based adjuvants of similar cationic charge, a high degree of antigen adsorption onto the adjuvants was achieved. Since NadA3 has a pI of 4.4 it was expected it would readily adsorb to the particle surfaces of the adjuvants evaluated in this work. High antigen-loading capacity is a desirable property of adjuvant particulates as it avoids antigen loss during the manufacturing process and further need of adjusting the injection volume of the final product to achieve the correct antigen concentration. This can simplify manufacture and reduces development costs. Generally, the co-formulation with NadA3 resulted in increases of liposome, solid lipid nanoparticle and polymeric nanoparticle sizes with reduced zeta potentials, while the emulsion size was less affected. Alteration in particle attributes after antigen adsorption has also been reported in the literature (37, 50). For example, immediate CAF01 liposome aggregation, increased polydispersity and reduced zeta potential was observed after protein antigen mixing (51). In contrast, studies with cationic nanoemulsions based on DOTAP:MF59 highlighted that antigen adsorption did not dramatically modify droplet sizes (54). The high colloidal stability of emulsions has been attributed to the presence of Tween 80. It is well documented that incorporation of nonionic surfactants with poly(ethylene glycol) moieties (PEG-lipid) increases the physical stability of formulations by increasing steric hindrance and preventing particle fusion by e.g. Ostwald Ripening (52).

In vitro, cationic liposomes, solid lipid nanoparticles and polymeric nanoparticles were readily associated with THP-1 cells, while emulsion internalization was less efficient. Although all formulations were cationic, emulsions had lower positive zeta potential and the presence of Tween 80, which in combination might lower the degree of cellular association. It is widely accepted that

595 cationic surface charge for most nanoparticles correlates with higher cellular uptake and trafficking,
596 owing to the electrostatic binding with negatively charged cell membrane (51, 53). Accordingly,
597 positively charged liposomes, solid lipid nanoparticles and polymeric nanoparticles would interact
598 more efficiently with cells *in vitro* compared to less positively charged emulsions. However, the
599 marked differences among formulations' cellular trafficking suggested that physicochemical factors
600 than other just electrostatic interactions were involved. We speculated that the four adjuvants
601 tested herein could have different elasticities based on physicochemical properties of the
602 components in the different formulations, although extensive evaluation of Young's modulus of
603 different formulations was not undertaken in the present work. Numerous studies that focused on
604 the impact of particle elasticity on cellular uptake, agreed on the preference of cells to better
605 internalize more rigid particles than softer counterparts (54, 55). Considering that emulsions were
606 composed mainly of excipients which were liquid at room temperature (e.g. squalene, Span 85 and
607 Tween 80), we expected them to be more fluid than liposomes, solid lipid nanoparticles or polymeric
608 nanoparticles, which contained excipients of high transition temperature (e.g. PLGA, tristearin and
609 DDA), and therefore less internalized by cells. Another fact that could have contributed to lower
610 emulsion association might be the presence of PEG on the droplets surface; indeed, the hydrophilic
611 steric barrier induced by poly(ethylene glycol) might hamper association with cell membranes thus
612 preventing cellular adsorption and internalization (56).
613 Association efficiency analysed as relative number of particles varied among adjuvants, with number
614 of associated liposomes > solid lipid nanoparticles >> polymeric nanoparticles and emulsions.
615 Differences observed could be related to differences in particle hydrodynamic radius, as Nr is
616 indirectly proportional to particle size; thus, despite comparable MFIs, liposomes which were
617 smaller in size would have higher Nr than solid lipid nanoparticles and polymeric nanoparticles.
618 Importantly, these findings suggested that smaller particles were better associated with cells than
619 larger counterparts. Similar results in macrophages were observed elsewhere, with an inverse
620 correlation between liposome size and their cell uptake *in vitro* when represented as number of
621 internalized vesicles (43, 57). The poor ability of emulsions to facilitate antigen processing (based
622 on antigen degradation) correlated with aforementioned association efficiency *in vitro*, as reduced
623 formulation accumulation within cells inevitably lowers the capture and degradation of associated
624 antigen (58). Nonetheless, the delivery of protein with liposomes, solid lipid nanoparticles and
625 polymeric nanoparticles clearly improved antigen degradation activity compared to the
626 unformulated control. In these studies, it was not possible to distinguish extracellular and

phagocytosed nanoparticles. Therefore, the biodistribution studies were used to indicate the presence of adjuvant at the injection site and possible drainage of intact particles to lymph nodes and other distal sites. Evaluation of the DiD signal on a cellular level, e.g. by confocal microscopy, might shed further light on the level of adjuvant uptake by cells in the tissue.

In vivo, the biodistribution of NadA3 adjuvanted with cationic liposomes, solid lipid nanoparticles and polymeric nanoparticles was comparable to adjuvants that show prolonged deposition in the injection site (59), while emulsions drained away faster. The depot effect is related to the attraction between the cationic surface charge and negatively charged serum proteins or components of the extracellular matrix (e.g. heparan sulfates), which cause aggregation and limited passive draining of the formulations to the rest of the body (60, 61). This longer permanency of particles at the injection site favours a continuous presentation of the antigen to the immune cells (18) and potentially increases immune response (62). Although our newly formulated adjuvants were all positively charged, their retention efficiency varied among formulations, thus suggesting that a cationic surface charge is not the only parameter, which dictates the pharmacokinetics of particles. The ineffective depot of emulsions reflected the poor cell association efficiency observed *in vitro* and could be due to the presence of PEGylated non-ionic surfactant in the outer layer of the emulsion droplets (63, 64), as rigid barriers (e.g. grafted polymer brush surfaces) or the modification of physicochemical attributes of particle surface (e.g. hydrophilicity/hydrophobicity) hamper serum protein adsorption efficiency *in vivo* with a consequent reduction of particle precipitation at the injection site (65). The effects of PEG polymer on biodistribution explored by using several colloidal systems has been shown to lower the retention of particles at the injection sites (64, 66, 67), while favouring their transportation to and retention in the lymphatics as a consequence of augmented passive drainage of particles (68). A study, which evaluated the biodistribution of the MF59 analogue AddaVax, showed fast initial clearance of the formulation from the leg muscle followed by constant adjuvant levels between 20 and 30% of injected dose detected up to 14 days post injection (69). From our studies, we see a similar kinetic profile, with an initial rapid drop in the levels of emulsion at the injection site followed by a similar kinetic profile for all the adjuvants. This maybe a result of the binding capacity of the tissue for the different adjuvant systems which, whilst all being similar in cationic nature, have different physical attributes. We also found that i.m. administration of radiolabeled DDA-based emulsions showed enhanced accumulation of droplets in the local draining lymph nodes over 48 hours as compared to DDA liposomes, SLNs or PNPs, which is consistent with the mechanism of action of MF59-like emulsions proposed in the literature (1).

Interestingly, the accumulation in the kidneys of NadA3 either unformulated or associated with cationic delivery systems was not significantly different, thus indicating that the delivery of antigen through a synthetic particulate did not alter protein metabolic profile. This finding might be useful when considering possible adverse events of local antigen delivery though synthetic particulates, e.g. liver toxicity due to particle aggregation. The association between cationic particulates and tissue components of the extracellular matrix could also promote release of adsorbed antigen, as suggested by the progressive decrease of NadA3 signal from the quadriceps and consequent accumulation in the kidneys observed within this work. This maybe the full antigen or digested antigen fragments. The formation of a depot at the injection site has been shown to be critical for the adjuvant effect of the DDA-based CAF01. Thus, an analogue based on the unsaturated dimethyldioleoylammonium chloride (DODA) did not form a depot at the injection site, which caused almost complete abrogation of the adaptive cell-mediated immune Th1/Th17 response (70). Furthermore, co-delivery of adjuvant and antigen to the same cell is required for induction of a cell-mediated immune response (71). Therefore, we hypothesized that efficient depot formation and cellular association might correlate with the ability to induce adaptive immune responses. However, induction of humoral immune responses does not necessarily require antigen processing and cellular activation at the injection site. Rather, targeting of germinal centers in the lymph nodes with intact protein antigen may contribute to the quality of the humoral immune responses, as unprocessed antigens increase the chances of the presence of good B cell epitopes (72).

Directly comparing the immunogenicity of cationic emulsions, liposomes, solid lipid nanoparticles and polymeric nanoparticles *in vivo* revealed that DDA-based emulsions were the most effective in eliciting high level of IgG antibody response (mainly IgG1) in mice, followed by liposomes. This is despite our in vitro studies suggesting low emulsion uptake and DQ-OVA degradation (which is suggested as a proxy for antigen processing). In contrast, the polymeric nanoparticles which promoted higher cell uptake and antigen degradation, failed to induce robust humoral responses (either total IgG or subclasses). Although the release mechanism of PLGA NPs was not investigated in the present study, we hypothesize that this lack of potency might be due to partial NadA3 denaturation by PLGA degradation products. It is widely accepted that, in an aqueous environment, PLGA undergoes hydrolysis of its ester bonds, through bulk or heterogeneous erosion (73). Consequently, lactic acid (LA) and glycolic acid (GA) are formed, which lower the pH of the environment. Acidification is known to cause protein denaturation by disruption of salt bridges on the amino acid backbone, which promote protein chain unfolding and affect protein biological

activity (74). The polymer degradation rate can be influenced by the ratio of GA to LA; usually PLGA with a higher content of LA are less hydrophilic and subsequently degrade more slowly (75). However, the copolymer 50:50 represents an exception to this rule, as faster degradation and accelerated production of acidic monomers is reported (75). Rapid degradation might be desirable as it increases polymer biocompatibility and safety by reducing its accumulation in different organs, although degradation products might affect the integrity of the chosen antigen. If that was the case, the drawback could be limited by tailoring the properties of the PLGA polymer to delay degradation or by incorporating basic salts in formulations to neutralize the acidic environment (76).

Overall, titers of antigen-specific IgG1 isotype were higher than those of IgG2a, suggesting a possible polarization toward a Th2 phenotype induced by adjuvanted NadA3. Furthermore, no detectable cell-mediated immune (CMI) responses were induced by any of the adjuvants tested. The lack of Th1 and CMI responses may be due to the lack of an immunostimulator as adjuvant component, e.g. a Toll-like receptor ligand, which has been shown to aid the induction of CMI responses. For example, the incorporation of the Mincle-agonist monomycoloyl glycerol (MMG) into DDA-based liposomes potentiated CMI responses, while a mild increase in the antigen-specific IgG2c antibody responses against a *M. tuberculosis* antigen was observed (77). Similarly, comparison of neat DDA and DDA:TDB-liposomes as adjuvants for a *M. tuberculosis* antigen confirmed the immunostimulatory activity of TDB, with augmented IFN-γ responses, while the IgG1 and IgG2c responses did not improve (18).

In general, our findings suggested that formulations which induced a depot effect were those which were less potent in eliciting efficient antigen-specific antibody responses. Accordingly, the adjuvant mechanism of MF59-like squalene-based emulsions has been found not to involve the formation of a depot but the creation of an immunocompetent environment at the site of administration which increases immune cell recruitment (i.e., antigen presenting cells) and antigen processing (78). It was reported that this elicited cellular infiltrate led to a large increase in total antibody titers (79). The results obtained for the emulsion in the present papers correlates with these findings. Moreover, many papers refer to an intracellular co-localization of antigen and adjuvant after intramuscular injection (80). This observation further supported the hypothesis that squalene-based emulsions directly increase phagocytosis and pinocytosis and promote antigen uptake by antigen presenting cells (81). Furthermore, MF59-like emulsions have been shown to favour retention of the protein antigen in the draining lymph node (82), which might also be the mechanism of action for the emulsion adjuvant evaluated herein .

Conclusions

In the present study, we demonstrated that the format of an adjuvant strongly influences *in vitro* cell association and antigen processing, *in vivo* pharmacokinetics and immunogenicity of four NadA3-adsorbing cationic formulations. Results reported here show that the co-formulation of cationic adjuvants and sub-unit antigen increased particle size from <130 nm up to 350 nm and reduced the positive surface charge of the adjuvants. Despite differences in physical attributes, all four formulations displayed high antigen adsorption efficiency. *In vitro,* emulsions induced low levels of cell association and antigen processing and did not promote a prolonged antigen deposition at the injection site *in vivo*, while comparable *in vitro* antigen trafficking and *in vivo* distribution was observed for liposomes, polymeric nanoparticles and solid lipid nanoparticles. However, the resulting humoral immune response was significantly different among the cationic formulations with total IgG production following the order emulsions > liposomes > solid lipid nanoparticles > polymeric nanoparticles. These results demonstrate that the the format of cationic adjuvants with matching cationic lipid content impact on the induction of antigen-specific antibody responses.

Acknowledgements.

This work was funded by the European Commission Project Leveraging Pharmaceutical Sciences and Structural Biology Training to Develop 21st 518 Century Vaccines (H2020-MSCA-ITN-2015 grant agreement 675370) and Independent Research Fund Denmark (7026-00027B) (S.S.). We wish to thank the staff at Biological Procedures Unit (BPU) at University of Strathclyde for technical assistance. The data that support the findings are openly available through the University of Strathclyde pure portal https://doi.org/10.15129/53542a9c-9b57-4498-b74d-ae98edc53135.

Conflicts of interest

Giulia Anderluzzi and Robert Cunliffe participated in the European Marie Curie PHA-ST-TRAIN-VAC PhD project at the University of Strathclyde (Glasgow, UK) in collaboration with GSK (Siena, Italy). This project was co-sponsored between the University of Strathclyde and GlaxoSmithKline Biologicals SA. Signe Tandrup Schmidt [Independent Research Fund Denmark (7026-00027B)], Yvonne Perrie, Stuart Woods, Craig W. Roberts declare no conflict of interest. Daniele Veggi, Ilaria Ferlenghi, Derek T. O'Hagan and Barbara C. Baudner are employees of the GSK group of companies. All other authors declare that they have no other relevant affiliations or financial interest in conflict with the subject matter or materials discussed in the manuscript.

Author contribution

Giulia Anderluzzi: Conceptualization, methodology, software, formal analysis, investigation, validation, resources, writing – original draft, writing – review and editing, visualization. Signe Tandrup Schmidt: Conceptualization, methodology, software, formal analysis, investigation, validation, resources, writing – review and editing, visualization. Robert Cunliffe: Methodology, formal analysis, validation, resources, writing – review and editing. Stuart Woods: Methodology, Craig W. Roberts: conceptualization, supervision, writing – review and editing, Daniele Veggi: Methodology, Ilaria Ferlenghi: conceptualization, supervision, writing – review and editing, Derek T. O'Hagan: conceptualization, supervision, writing – review and editing, Barbara C. Baudner: Conceptualization, methodology, validation, resources, writing – review and editing, supervision, funding acquisition and project management of PHA-ST-TRAIN-VAC. Yvonne Perrie: Conceptualization, methodology, validation, resources, writing – review and editing, visualization, supervision, funding acquisition and project management of PHA-ST-TRAIN-VAC. All authors reviewed and approved the final draft of the manuscript.

References

1. O'Hagan DT, Ott GS, De Gregorio E, Seubert A. The mechanism of action of MF59 - an innately attractive adjuvant formulation. Vaccine. 2012;30(29):4341-8.
2. O'Hagan DT, Tsai TF, Brito LA. Emulsion based vaccine adjuvants. Human Vaccines & Immunotherapeutics. 2013;9(8):1698-700.
3. Khurana S, Coyle EM, Manischewitz J, King LR, Gao J, Germain RN, et al. AS03-adjuvanted H5N1 vaccine promotes antibody diversity and affinity maturation, NAI titers, cross-clade H5N1 neutralization, but not H1N1 cross-subtype neutralization. npj Vaccines. 2018;3(1):40.
4. Wang N, Chen M, Wang T. Liposomes used as a vaccine adjuvant-delivery system: From basics to clinical immunization. J Control Release. 2019;303:130-50.
5. Jain S, O'Hagan DT, Singh M. The long-term potential of biodegradable poly(lactide-co-glycolide) microparticles as the next-generation vaccine adjuvant. Expert Rev Vaccines. 2011;10(12):1731-42.
6. Eldridge JH, Staas JK, Meulbroek JA, Tice TR, Gilley RM. Biodegradable and biocompatible poly(DL-lactide-co-glycolide) microspheres as an adjuvant for staphylococcal enterotoxin B toxoid which enhances the level of toxin-neutralizing antibodies. Infect Immun. 1991;59(9):2978-86.
7. Roces CB, Christensen D, Perrie Y. Translating the fabrication of protein-loaded poly(lactic-co-glycolic acid) nanoparticles from bench to scale-independent production using microfluidics. Drug Deliv Transl Res. 2020.
8. Roces CB, Hussain MT, Schmidt ST, Christensen D, Perrie Y. Investigating Prime-Pull Vaccination through a Combination of Parenteral Vaccination and Intranasal Boosting. Vaccines (Basel). 2019;8(1).
9. Klinguer C, Beck A, De-Lys P, Bussat MC, Blaecke A, Derouet F, et al. Lipophilic quaternary ammonium salt acts as a mucosal adjuvant when co-administered by the nasal route with vaccine antigens. Vaccine. 2001;19(30):4236-44.
10. Lima KM, Bonato VLD, Faccioli LH, Brandão IrT, dos Santos SA, Coelho-Castelo AAM, et al. Comparison of different delivery systems of vaccination for the induction of protection against tuberculosis in mice. Vaccine. 2001;19(25):3518-25.
11. Tsuruta L, Quintilio W, Costa MH, Carmonaribeiro A. Interactions between cationic liposomes and an antigenic protein: The physical chemistry of the immunoadjuvant action. Journal of lipid research. 1997;38:2003-11.
12. Chan C-L, Ewert KK, Majzoub RN, Hwu Y-K, Liang KS, Leal C, et al. Optimizing cationic and neutral lipids for efficient gene delivery at high serum content. The journal of gene medicine. 2014;16(3-4):84-96.
13. Sedighi M, Sieber S, Rahimi F, Shahbazi M-A, Rezayan ah, Huwyler J, et al. Rapid optimization of liposome characteristics using a combined microfluidics and design-of-experiment approach. Drug Deliv Transl Res. 2018;9.
14. Tandrup Schmidt S, Foged C, Korsholm KS, Rades T, Christensen D. Liposome-Based Adjuvants for Subunit Vaccines: Formulation Strategies for Subunit Antigens and Immunostimulators. Pharmaceutics. 2016;8(1):7.
15. Pérez-Betancourt Y, Távora BCLF, Colombini M, Faquim-Mauro EL, Carmona-Ribeiro AM. Simple nanoparticles from the assembly of cationic polymer and antigen as immunoadjuvants. Vaccines. 2020;8(1):105.
16. Gall D. The adjuvant activity of aliphatic nitrogenous bases. Immunology. 1966;11(4):369-86.
17. Milicic A, Kaur R, Reyes-Sandoval A, Tang C-K, Honeycutt J, Perrie Y, et al. Small cationic DDA:TDB liposomes as protein vaccine adjuvants obviate the need for TLR agonists in inducing cellular and humoral responses. PLoS One. 2012;7(3):e34255-e.
18. Henriksen-Lacey M, Bramwell VW, Christensen D, Agger EM, Andersen P, Perrie Y. Liposomes based on dimethyldioctadecylammonium promote a depot effect and enhance immunogenicity of soluble antigen. J Control Release. 2010;142(2):180-6.
19. Hilgers LAT, Snippe H, Jansze M, Willers JMN. Combinations of two synthetic adjuvants: Synergistic effects of a surfactant and a polyanion on the humoral immune response. Cellular Immunology. 1985;92(2):203-9.
20. Korsholm KS, Agger EM, Foged C, Christensen D, Dietrich J, Andersen CS, et al. The adjuvant mechanism of cationic dimethyldioctadecylammonium liposomes. Immunology. 2007;121(2):216-26.
21. Banchereau J, Steinman RM. Dendritic cells and the control of immunity. Nature. 1998;392(6673):245-52.
22. Brito LA, Chan M, Shaw CA, Hekele A, Carsillo T, Schaefer M, et al. A Cationic Nanoemulsion for the Delivery of Next-generation RNA Vaccines. Mol Ther. 2014;22(12):2118-29.
23. Bogers WM, Oostermeijer H, Mooij P, Koopman G, Verschoor EJ, Davis D, et al. Potent Immune Responses in Rhesus Macaques Induced by Nonviral Delivery of a Self-amplifying RNA Vaccine Expressing HIV Type 1 Envelope With a Cationic Nanoemulsion. Journal of Infectious Diseases. 2014.
24. Wusiman A, Gu P, Liu Z, Xu S, Zhang Y, Hu Y, et al. Cationic polymer modified PLGA nanoparticles encapsulating Alhagi honey polysaccharides as a vaccine delivery system for ovalbumin to improve immune responses. Int J Nanomedicine. 2019;14:3221-34.

25. Khademi F, Yousefi-Avarvand A, Derakhshan M, Abbaspour MR, Sadri K, Tafaghodi M. Formulation and Optimization of a New Cationic Lipid-Modified PLGA Nanoparticle as Delivery System for Mycobacterium tuberculosis HspX/EsxS Fusion Protein: An Experimental Design. IIran J Pharm Res. 2019;18(1):446-58.
26. Qi C, Chen Y, Huang JH, Jin QZ, Wang XGJJotSoF, 92 AV. Preparation and characterization of catalase-loaded solid lipid nanoparticles based on soybean phosphatidylcholine. 2012(4):787-93.
27. Becker Peres L, Becker Peres L, de Araújo PHH, Sayer C. Solid lipid nanoparticles for encapsulation of hydrophilic drugs by an organic solvent free double emulsion technique. Colloids and Surfaces B: Biointerfaces. 2016;140:317-23.
28. Zhang Q, Yie G, Li Y, Yang Q, Nagai T. Studies on the cyclosporin A loaded stearic acid nanoparticles. International Journal of Pharmaceutics. 2000;200(2):153-9.
29. Ugazio E, Cavalli R, Gasco MR. Incorporation of cyclosporin A in solid lipid nanoparticles (SLN). International Journal of Pharmaceutics. 2002;241(2):341-4.
30. Pardeike J, Schwabe K, Müller RH. Influence of nanostructured lipid carriers (NLC) on the physical properties of the Cutanova Nanorepair Q10 cream and the in vivo skin hydration effect. Int J Pharm. 2010;396(1):166-73.
31. Souto EB, Müller RH. SLN and NLC for topical delivery of ketoconazole. J Microencapsul. 2005;22(5):501-10.
32. Masignani V, Pizza M, Moxon ER. The Development of a Vaccine Against Meningococcus B Using Reverse Vaccinology. Front Immunol. 2019;10:751.
33. Capecchi B, Adu-Bobie J, Di Marcello F, Ciucchi L, Masignani V, Taddei A, et al. Neisseria meningitidis NadA is a new invasin which promotes bacterial adhesion to and penetration into human epithelial cells. Molecular Microbiology. 2005;55(3):687-98.
34. Bowe F, Lavelle EC, McNeela EA, Hale C, Clare S, Arico B, et al. Mucosal vaccination against serogroup B meningococci: induction of bactericidal antibodies and cellular immunity following intranasal immunization with NadA of Neisseria meningitidis and mutants of Escherichia coli heat-labile enterotoxin. Infect Immun. 2004;72(7):4052-60.
35. Litt DJ, Savino S, Beddek A, Comanducci M, Sandiford C, Stevens J, et al. Putative Vaccine Antigens from Neisseria meningitidis Recognized by Serum Antibodies of Young Children Convalescing after Meningococcal Disease. The Journal of Infectious Diseases. 2004;190(8):1488-97.
36. Liguori A, Dello Iacono L, Maruggi G, Benucci B, Merola M, Lo Surdo P, et al. NadA3 Structures Reveal Undecad Coiled Coils and LOX1 Binding Regions Competed by Meningococcus B Vaccine-Elicited Human Antibodies. mBio. 2018;9(5):e01914-18.
37. Ott G, Singh M, Kazzaz J, Briones M, Soenawan E, Ugozzoli M, et al. A cationic sub-micron emulsion (MF59/DOTAP) is an effective delivery system for DNA vaccines. Journal of Controlled Release. 2002;79(1):1-5.
38. Anderluzzi G, Lou G, Gallorini S, Brazzoli M, Johnson R, O'Hagan DT, et al. Investigating the Impact of Delivery System Design on the Efficacy of Self-Amplifying RNA Vaccines. Vaccines (Basel). 2020;8(2).
39. Henriksen-Lacey M, Bramwell V, Perrie Y. Radiolabelling of Antigen and Liposomes for Vaccine Biodistribution Studies. Pharmaceutics. 2010;2(2):91-104.
40. Roces CB, Khadke S, Christensen D, Perrie Y. Scale-Independent Microfluidic Production of Cationic Liposomal Adjuvants and Development of Enhanced Lymphatic Targeting Strategies. Molecular Pharmaceutics. 2019;16(10):4372-86.
41. Frey A, Di Canzio J, Zurakowski D. A statistically defined endpoint titer determination method for immunoassays. Journal of Immunological Methods. 1998;221(1):35-41.
42. Chatzikleanthous D, Schmidt ST, Buffi G, Paciello I, Cunliffe R, Carboni F, et al. Design of a novel vaccine nanotechnology-based delivery system comprising CpGODN-protein conjugate anchored to liposomes. Journal of Controlled Release. 2020.
43. Lou G, Anderluzzi G, Woods S, Roberts CW, Perrie Y. A novel microfluidic-based approach to formulate size-tuneable large unilamellar cationic liposomes: Formulation, cellular uptake and biodistribution investigations. European Journal of Pharmaceutics and Biopharmaceutics. 2019;143:51-60.
44. Malito E, Biancucci M, Faleri A, Ferlenghi I, Scarselli M, Maruggi G, et al. Structure of the meningococcal vaccine antigen NadA and epitope mapping of a bactericidal antibody. Proceedings of the National Academy of Sciences. 2014;111(48):17128-33.
45. Christensen D, Korsholm KS, Andersen P, Agger EM. Cationic liposomes as vaccine adjuvants. Expert Rev Vaccines. 2011;10(4):513-21.
46. Black M, Trent A, Tirrell M, Olive C. Advances in the design and delivery of peptide subunit vaccines with a focus on toll-like receptor agonists. Expert review of vaccines. 2010;9(2):157-73.
47. Kopatz I, Remy J-S, Behr J-P. A Model for Non-Viral Gene Delivery: Through Syndecan Adhesion Molecules and Powered by Actin. The journal of gene medicine. 2004;6:769-76.
48. Hafez I, Maurer N, Cullis P. On the mechanism whereby cationic lipids promote intracellular delivery of polynucleic acids. Gene therapy. 2001;8:1188-96.

882 49. Hamborg M, Jorgensen L, Bojsen A, Christensen D, Foged C. Protein antigen adsorption to the DDA/TDB
883 liposomal adjuvant: Effect on protein structure, stability, and liposome physicochemical characteristics. Pharm Res.
884 2013;30(1):140-55.
885 50. Henriksen-Lacey M, Devitt A, Perrie Y. The vesicle size of DDA:TDB liposomal adjuvants plays a role in the cell-
886 mediated immune response but has no significant effect on antibody production. J Control Release. 2011;154(2):131-
887 7.
888 51. Henriksen-Lacey M, Christensen D, Bramwell VW, Lindenstrom T, Agger EM, Andersen P, et al. Liposomal
889 cationic charge and antigen adsorption are important properties for the efficient deposition of antigen at the injection
890 site and ability of the vaccine to induce a CMI response. J Control Release. 2010;145(2):102-8.
891 52. Taylor P. Ostwald ripening in emulsions: estimation of solution thermodynamics of the disperse phase. Adv
892 Colloid Interface Sci. 2003;106:261-85.
893 53. Inglut CT, Sorrin AJ, Kuruppu T, Vig S, Cicalo J, Ahmad H, et al. Immunological and Toxicological
894 Considerations for the Design of Liposomes. Nanomaterials (Basel). 2020;10(2):190.
895 54. Foroozandeh P, Aziz AA. Insight into Cellular Uptake and Intracellular Trafficking of Nanoparticles. Nanoscale
896 Res Lett. 2018;13(1):339-.
897 55. Li Z, Xiao C, Yong T, Li Z, Gan L, Yang X. Influence of nanomedicine mechanical properties on tumor targeting
898 delivery. Chemical Society reviews. 2020;49(8):2273-90.
899 56. Suk JS, Xu Q, Kim N, Hanes J, Ensign LM. PEGylation as a strategy for improving nanoparticle-based drug and
900 gene delivery. Adv Drug Deliv Rev. 2016;99(Pt A):28-51.
901 57. Ahsan F, Rivas IP, Khan MA, Torres Suarez AI. Targeting to macrophages: role of physicochemical properties
902 of particulate carriers--liposomes and microspheres--on the phagocytosis by macrophages. J Control Release.
903 2002;79(1-3):29-40.
904 58. Patil NS, Wong DL, Collier KD, McDonald HC. Fluorescent derivatization of a protease antigen to track antigen
905 uptake and processing in human cell lines. BMC Immunology. 2004;5(1):12.
906 59. Henriksen-Lacey M, Christensen D, Bramwell VW, Lindenstrøm T, Agger EM, Andersen P, et al. Comparison of
907 the depot effect and immunogenicity of liposomes based on dimethyldioctadecylammonium (DDA), 3β-[N-(N',N'-
908 Dimethylaminoethane)carbomyl] cholesterol (DC-Chol), and 1,2-Dioleoyl-3-trimethylammonium propane (DOTAP):
909 prolonged liposome retention mediates stronger Th1 responses. Mol Pharm. 2011;8(1):153-61.
910 60. De Serrano LO, Burkhart DJ. Liposomal vaccine formulations as prophylactic agents: design considerations for
911 modern vaccines. Journal of Nanobiotechnology. 2017;15(1):83.
912 61. Nisini R, Poerio N, Mariotti S, De Santis F, Fraziano M. The Multirole of Liposomes in Therapy and Prevention
913 of Infectious Diseases. Frontiers in Immunology. 2018;9(155).
914 62. Hussain MJ, Wilkinson A, Bramwell VW, Christensen D, Perrie Y. Th1 immune responses can be modulated by
915 varying dimethyldioctadecylammonium and distearoyl-sn-glycero-3-phosphocholine content in liposomal adjuvants. J
916 Pharm Pharmacol. 2014;66(3):358-66.
917 63. Nunes SS, Fernandes RS, Cavalcante CH, da Costa César I, Leite EA, Lopes SCA, et al. Influence of PEG coating
918 on the biodistribution and tumor accumulation of pH-sensitive liposomes. Drug Deliv Transl Res. 2019;9(1):123-30.
919 64. Schmidt ST, Olsen CL, Franzyk H, Wørzner K, Korsholm KS, Rades T, et al. Comparison of two different
920 PEGylation strategies for the liposomal adjuvant CAF09: Towards induction of CTL responses upon subcutaneous
921 vaccine administration. Eur J Pharm Biopharm. 2019;140:29-39.
922 65. Walkey CD, Chan WC. Understanding and controlling the interaction of nanomaterials with proteins in a
923 physiological environment. Chem Soc Rev. 2012;41(7):2780-99.
924 66. Zhuang Y, Ma Y, Wang C, Hai L, Yan C, Zhang Y, et al. PEGylated cationic liposomes robustly augment vaccine-
925 induced immune responses: Role of lymphatic trafficking and biodistribution. J Control Release. 2012;159(1):135-42.
926 67. Xue W, Liu Y, Zhang N, Yao Y, Ma P, Wen H, et al. Effects of core size and PEG coating layer of iron oxide
927 nanoparticles on the distribution and metabolism in mice. Int J Nanomedicine. 2018;13:5719-31.
928 68. Zhan X, Tran KK, Shen H. Effect of the poly(ethylene glycol) (PEG) density on the access and uptake of
929 particles by antigen-presenting cells (APCs) after subcutaneous administration. Mol Pharm. 2012;9(12):3442-51.
930 69. Tegenge MA, Von Tungeln LS, Anderson SA, Mitkus RJ, Vanlandingham MM, Forshee RA, et al. Comparative
931 pharmacokinetic and biodistribution study of two distinct squalene-containing oil-in-water emulsion adjuvants in
932 H5N1 influenza vaccines. Regulatory Toxicology and Pharmacology. 2019;108:104436.
933 70. Christensen D, Henriksen-Lacey M, Kamath AT, Lindenstrøm T, Korsholm KS, Christensen JP, et al. A cationic
934 vaccine adjuvant based on a saturated quaternary ammonium lipid have different in vivo distribution kinetics and
935 display a distinct CD4 T cell-inducing capacity compared to its unsaturated analog. J Control Release. 2012;160(3):468-
936 76.
937 71. Kamath AT, Mastelic B, Christensen D, Rochat A-F, Agger EM, Pinschewer DD, et al. Synchronization of
938 dendritic cell activation and antigen exposure is required for the induction of Th1/Th17 responses. J Immunol.
939 2012;188(10):4828-37.

72. Calabro S, Tortoli M, Baudner BC, Pacitto A, Cortese M, O'Hagan DT, et al. Vaccine adjuvants alum and MF59 induce rapid recruitment of neutrophils and monocytes that participate in antigen transport to draining lymph nodes. Vaccine. 2011;29(9):1812-23.
73. Engineer C, Parikh J, Raval A. Review on Hydrolytic Degradation Behavior of Biodegradable Polymers from Controlled Drug Delivery System. Trends in Biomaterials and Artificial Organs. 2011;25.
74. Hines DJ, Kaplan DL. Poly(lactic-co-glycolic) acid-controlled-release systems: experimental and modeling insights. Crit Rev Ther Drug Carrier Syst. 2013;30(3):257-76.
75. Wu XS, Wang N. Synthesis, characterization, biodegradation, and drug delivery application of biodegradable lactic/glycolic acid polymers. Part II: biodegradation. Journal of biomaterials science Polymer edition. 2001;12(1):21-34.
76. Giteau A, Venier-Julienne MC, Aubert-Pouessel A, Benoit JP. How to achieve sustained and complete protein release from PLGA-based microparticles? Int J Pharm. 2008;350(1-2):14-26.
77. Nordly P, Korsholm KS, Pedersen EA, Khilji TS, Franzyk H, Jorgensen L, et al. Incorporation of a synthetic mycobacterial monomycoloyl glycerol analogue stabilizes dimethyldioctadecylammonium liposomes and potentiates their adjuvant effect in vivo. Eur J Pharm Biopharm. 2011;77(1):89-98.
78. O'Hagan D. The history of MF59® adjuvant: a phoenix that arose from the ashes. 2013.
79. Vono M, Taccone M, Caccin P, Gallotta M, Donvito G, Falzoni S, et al. The adjuvant MF59 induces ATP release from muscle that potentiates response to vaccination. Proc Natl Acad Sci U S A. 2013;110(52):21095-100.
80. Didierlaurent AM, Laupèze B, Di Pasquale A, Hergli N, Collignon C, Garçon N. Adjuvant system AS01: helping to overcome the challenges of modern vaccines. Expert Review of Vaccines. 2017;16(1):55-63.
81. Seubert A, Monaci E, Pizza M, O'Hagan D, Wack A. The ADJUVANTS ALUMINUM HYDROXIDE and MF59 induce monocyte and granulocyte chemoattractants and enhance monocyte differentiation toward dendritic cells. Journal of immunology (Baltimore, Md : 1950). 2008;180:5402-12.
82. Cantisani R, Pezzicoli A, Cioncada R, Malzone C, De Gregorio E, D'Oro U, et al. Vaccine adjuvant MF59 promotes retention of unprocessed antigen in lymph node macrophage compartments and follicular dendritic cells. J Immunol. 2015;194(4):1717-25.

Tables

Table 1. Physicochemical properties of DDA-based formulations. Chemical composition, size (z-average), polydispersity index (PDI), zeta potential (ZP) and NadA3 adsorbance efficiency (A. E.) of DDA-based emulsions, solid lipid nanoparticles, polymeric nanoparticles and liposomes either in presence or in absence of 100 µg/mL of NadA3 antigen. DDA: Dimethyldioctadecylammonium bromide, PLGA: poly(lactic-co-glycolic acid), DOPE: dioleoylphosphatidylethanolamine. Results are represented as mean ± SD of three independent measurements, * $p \leq 0.05$ significance between formulations prepared with and without NadA3.

Delivery system	Chemical composition (mg/mL)	NadA3 protein (µg/mL)	Size ± SD (d.nm)	PDI ± SD	ZP ± SD (mV)	NadA3 A.E. ± SD (%)
Emulsions	Squalene: 3.5 DDA: 3.0 Span 85: 0.3 Tween 80: 0.3	0	131 ± 18	0.18 ± 0.02	28 ± 3	-
		100	187 ± 6*	0.22±0.02	19 ± 2*	92 ± 2
Liposomes	DOPE: 3.0 DDA: 3.0	0	41 ± 4	0.25 ±0.01	56 ± 4	-
		100	111 ± 4*	0.39±0.01*	37 ± 2*	95 ± 2
Polymeric nanoparticles	PLGA: 3.0 DDA: 3.0	0	38 ± 3	0.11±0.03	53 ± 2	-
		100	356 ± 81*	0.17±0.03	41± 7*	95 ± 1
Solid lipid nanoparticles	Tristearin: 3.0 DDA: 3.0	0	66 ± 2	0.15±0.03	43± 5	-
		100	154 ± 4*	0.37±0.02*	31 ± 5*	85 ± 1

Figure Legends

Figure 1. *In vitro* association of adjuvants with THP-1 cells and induction of antigen degradation. Association efficiency of emulsions, liposomes, polymeric nanoparticles (PNPs) or solid lipid nanoparticles (SLNs) expressed as A) Percentage of DiD^+ cells, B) DiD mean florescence intensity (MFI) or C) Relative number of associated adjuvants (Nr). Antigen degradation efficiency of emulsions, liposomes, PNPs or SLNs is expressed as D) DQ-OVA^+ cells and E) DQ-OVA mean fluorescence intensity (MFI). F) Plots the % of cell association versus % antigen processing at all time points measured (data from A and D). Results are represented as mean ± SD of three independent experiments. Refer to Figure S1 in the supplementary for representative histograms of DiD and DQ-OVA positive THP-1 cells incubated with different adjuvants.

Figure 2. Biodistribution of DiD-labelled adjuvants in mice following intramuscular administration. Female BALB/c mice were administered NadA3 adjuvanted with DiD-labelled emulsions, liposomes, polymeric nanoparticles (PNPs) and solid lipid nanoparticles (SLNs) intramuscularly in the right quadricep. The fluorescent signals were evaluated by IVIS over 11 days p.i. A) Pharmacokinetic profiles of DiD-labelled adjuvants at the injection site. B) Results were normalized and replotted as percentage of signal ratio. C) Images acquired at selected time points. Results are represented as the mean ± SD of three animals per group. Refer to Figure S2 in the supplementary for images of mice administered with adjuvanted NadA3 acquired at all time points over 11 days p.i.

Figure 3. Biodistribution of adjuvanted NadA3 antigen. Female BALB/c mice were administered unadjvuanted AF790-labelled NadA3 or adjuvanted with DiD-labelled emulsions, liposomes, polymeric nanoparticles (PNPs) and solid lipid nanoparticles (SLNs) intramuscularly in the right quadricep. The fluorescent signals were evaluated by IVIS over 11 days p.i. A) Pharmacokinetic profiles of either unadjuvanted or adjuvanted NadA3 at the injection site. B) Results were normalized and replotted as percentage of signal ratio. C) Images acquired at selected time points. Results are represented as the mean ± SD of three animals per group. Refer to Figure S3 in the supplementary for images of mice administered with either unadjuvanted or adjuvanted NadA3 acquired at all time points over 11 days p.i.

Figure 4. Comparison of AUC for both antigen and adjuvant after intramuscular injection. The retention of the antigen promoted by the adjuvant was calculated as area under the curve (AUC) for each formulation for both adjuvant and antigen (AUC; flux.day).

Figure 5. Biodistribution of radiolabeled cationic formulations. Female BALB/c mice were administered ^{3}H-cholesterol-labelled emulsions, liposomes, polymeric nanoparticles (PNPs) and solid lipid nanoparticles (SLNs) intramuscularly in the right quadriceps. The radioactivity was evaluated in the injection site, liver, spleen, popliteal lymph node (PLN), inguinal lymph node (ILN) and whole carcass over 48 hours p.i. A) Pharmacokinetic profiles of ^{3}H-cholesterol-labelled adjuvants. Percentage of dose determined at B) popliteal lymph node (PLN) and C) inguinal lymph node (ILN). Results are expressed as the mean ± SD of four animals. Data of biodistribution of liposomes were previously published by (43).

Figure 6. *In vivo* humoral responses promoted by four different cationic delivery platforms. Female BALB/c mice were immunized twice i.m. with unadjuvanted NadA3 (10 µg/dose) or NadA3 adjuvanted with cationic emulsions, liposomes, polymer nanoparticles (PNPs) and solid lipid nanoparticles (SLNs), with a booster immunization four weeks after the prime immunization. The antigen-specific total IgG, IgG1 and IgG2a levels in the blood were evaluated two weeks after the final immunization by using ELISA. Antigen specific A) total IgG levels, B) IgG1 and C) IgG2a average of mice in repeated studies, n=3-6, mean ± SD and end point titers for D) total IgG, E) IgG1 and F) IgG2a, n=4-6, lines denote mean ± SD. $p \leq 0.05$ (*).